See related commentary on pg 1514

Wnt/β-Catenin Signaling Stabilizes Hemidesmosomes in Keratinocytes

Hideyuki Kosumi[1], Mika Watanabe[1,2,3], Satoru Shinkuma[4], Takuma Nohara[1], Yu Fujimura[1], Tadasuke Tsukiyama[5], Giacomo Donati[2,3], Hiroaki Iwata[1], Hideki Nakamura[1], Hideyuki Ujiie[1] and Ken Natsuga[1]

Hemidesmosomes (HDs) are adhesion complexes that promote epithelial–stromal attachment in stratified and complex epithelia, including the epidermis. In various biological processes, such as differentiation and migration of epidermal keratinocytes during wound healing or carcinoma invasion, quick assembly and disassembly of HDs are prerequisites. In this study, we show that inhibition of Wnt/β-catenin signaling disturbs HD organization in keratinocytes. Screening with inhibitors identified the depletion of HD components and HD-like structures through Wnt inhibition, but keratinocyte differentiation was not affected. Wnt inhibition significantly diminished plectin and type XVII collagen expression in the basal side of Wnt-inhibited cells and the dermo–epidermal junction of the Wnt-inactive murine basal epidermis. Similar to Wnt inhibition, *PLEC*-knockout cells or cells with plectin–type XVII collagen binding defects showed type XVII collagen reduction in the basal side of the cells, implying the possible involvement of Wnt/β-catenin signaling in HD assembly. Atypical protein kinase C inhibition ameliorated the phenotypes of Wnt-inhibited cells. These findings show that Wnt/β-catenin signaling regulates the localization of HD components in keratinocytes and that the atypical protein kinase C pathway is involved in Wnt inhibition–induced HD disarrangement. Our study suggests that the Wnt signaling pathway could be a potential therapeutic target for treating HD-defective diseases, such as epidermolysis bullosa.

Journal of Investigative Dermatology (2022) **142,** 1576–1586; doi:10.1016/j.jid.2021.10.018

INTRODUCTION

In the skin, basal keratinocytes (KCs) are firmly attached to the underlying basement membrane through electron-dense structures called hemidesmosomes (HDs) (Borradori and Sonnenberg, 1999; Litjens et al., 2006). HDs provide stable adhesion of the epidermis to the dermis, resulting in skin stability against mechanical stress (Litjens et al., 2006; Natsuga et al., 2019; Zuidema et al., 2020). The epidermal attachment to the dermis through HDs in normal skin is destroyed only under extreme conditions, such as burns (Chetty et al., 1992) and suction blistering (Fujimura et al., 2021; Kiistala and Mustakallio, 1967; Krawczyk, 1971). Skin HDs contain plectin (PCN), BP230, type XVII collagen (COL17), and integrin α6 or β4 subunits (Borradori and Sonnenberg, 1999; Litjens et al., 2006). These proteins are essential for HD assembly and for maintenance of skin integrity on the basis of the following points: (i) genetically modified mice deficient in either of these proteins show loss of or greatly diminished HDs in the skin (Andrä et al., 1997; Dowling et al., 1996; Georges-Labouesse et al., 1996; Nishie et al., 2007; Raymond et al., 2005) and (ii) disease-causing sequence variants in the genes encoding these proteins (*PLEC*, *DST*, *COL17A1*, *ITGA6*, and *ITGB4*) are responsible for simplex or junctional subtypes of epidermolysis bullosa (EB), a group of skin fragility disorders in humans (Has et al., 2020a).

Notably, even when the expression of these proteins is maintained, faulty interactions among them lead to EB phenotypes. For example, missense variants in the PCN-binding region of the β4-integrin cause junctional EB (Koster et al., 2001; Nakano et al., 2001). Furthermore, the intracytoplasmic in-frame deletion of COL17, which prevents the association of COL17 with PCN, β4-integrin, and BP230, leads to EB simplex (Fontao et al., 2004), and one amino acid deletion in the COL17-binding domain of PCN is also causal for EB simplex (Natsuga et al., 2017). In line with these genetic studies, in vitro and biochemical experiments have shown that COL17-null cultured KCs fail to incorporate PCN into HD-like structures (Koster et al., 2003) and that the phosphorylation of β4-integrin destabilizes the interaction between β4-integrin and PCN, thereby initiating HD disassembly (Frijns et al., 2012, 2010). These studies indicate that the expression of HD proteins and their proper interactions are pivotal for HD formation. However, the spatial regulation of HD proteins has not been fully elucidated.

[1]*Department of Dermatology, Faculty of Medicine and Graduate School of Medicine, Hokkaido University, Sapporo, Japan;* [2]*Department of Life Sciences and Systems Biology, University of Turin, Turin, Italy;* [3]*Molecular Biotechnology Centre, University of Turin, Turin, Italy;* [4]*Department of Dermatology, Nara Medical University School of Medicine, Kashihara, Japan; and* [5]*Department of Biochemistry, Faculty of Medicine and Graduate School of Medicine, Hokkaido University, Sapporo, Japan*

Correspondence: Ken Natsuga, Department of Dermatology, Faculty of Medicine and Graduate School of Medicine, Hokkaido University, N15 W7, Sapporo 060-8638, Japan. E-mail: natsuga@med.hokudai.ac.jp

Abbreviations: aPKC, atypical protein kinase C; COL17, type XVII collagen; DEJ, dermo–epidermal junction; EB, epidermolysis bullosa; HD, hemidesmosome; IF, immunofluorescence; KC, keratinocyte; KO, knockout; NHEK, normal human epidermal keratinocyte; PCN, plectin; PKC, protein kinase C

Received 1 July 2021; revised 16 October 2021; accepted 24 October 2021; accepted manuscript published online 3 November 2021; corrected proof published online 24 November 2021

Wnt/β-catenin signaling is a crucial pathway that regulates skin morphogenesis and homeostasis (Lim and Nusse, 2013; Lu and Fuchs, 2014). Activating and inactivating sequence variants of Wnt/β-catenin signaling molecules result in distinct phenotypes showing proliferation and differentiation in murine skin KCs (Lim and Nusse, 2013). Our group has previously shown that COL17, an HD component, modulates epidermal proliferation by stabilizing Wnt/β-catenin signaling (Watanabe et al., 2017). In this study, by employing Wnt-inhibited cultured cells and mice, we found that the Wnt/β-catenin signaling pathway stabilizes the distribution of HD components in epidermal KCs.

RESULTS

Wnt inhibition reduces HD components in vitro

We first investigated the response of cultured epidermal cells to Wnt ligand treatment. Nonphosphorylated β-catenin (Ser33/37/Thr41), which is the active form of β-catenin and binds to LEF1 in the nucleus to invoke the canonical Wnt pathway (Lien et al., 2014), was hardly observed in the whole-cell lysates of normal human epidermal KCs (NHEKs) at steady state. Treatment with Wnt3a ligand, a canonical Wnt activator (Bryja et al., 2007), increased the activity of β-catenin in NHEKs (Supplementary Figure S1a). Unexpectedly, active β-catenin was abundant in HaCaT cells (an immortalized human KC cell line), irrespective of Wnt3a treatment (Supplementary Figure S1a), suggesting that Wnt/β-catenin signaling is constitutively active in HaCaT cells. HaCaT cells were then treated with Wnt inhibitors, Wnt C59 and ICG-001 (Supplementary Figure S1b). With Wnt C59 treatment, the amount of active β-catenin was reduced in a dose-dependent manner (Supplementary Figure S1b and c). In contrast, the reduction of activated β-catenin was not evident with ICG-001 (Supplementary Figure 1b and c) because the chemical antagonizes β-catenin/T-cell factors–mediated transcription that is downstream of canonical Wnt signaling (Emami et al., 2004). Downregulation of Wnt-target genes was confirmed in HaCaT cells treated with ICG-001 (Supplementary Figure S1d). Comparison of transcript levels between HaCaT cells and NHEKs revealed that most of the Wnt receptor genes and *AXIN2,* which encodes the critical regulator of the canonical Wnt pathway, were highly expressed in HaCaT cells (Supplementary Figure S1e).

Given Wnt activity in HaCaT cells, we sought to discover the molecules regulated by canonical Wnt pathways. Wnt inhibitor treatment (Wnt C59 or ICG-001) did not significantly affect the soluble fractions of HaCaT cell lysates in SDS-PAGE, followed by coomassie brilliant blue staining (Figure 1a and Supplementary Figure S2a). In contrast, Wnt inhibitors reduced some bands of HD-rich fractions of HaCaT cells, especially the band migrating far above 250 kDa (Figure 1b and Supplementary Figure S2b). Mass spectrometric analysis of the protein (the combination of Fourier transform mass spectrometry and ion trap tandem mass spectrometry) revealed that the most likely protein was PCN (score: 26.04). Immunoblots confirmed the reduction of PCN in the HD-rich fraction but not in the soluble fraction of HaCaT cells treated with Wnt inhibitors (Figure 1c and d). Wnt inhibitors also diminished the bands of COL17 and BP230, both of which are PCN-binding partners (Koster et al., 2003; Natsuga et al., 2017), in the HD-rich fraction but not in the soluble fraction of HaCaT cells (Figure 1c and d). Intriguingly, β4-integrin, another PCN-binding partner (Geerts et al., 1999), was not altered in either the soluble or HD-rich fractions. RT-qPCR showed that Wnt inhibitors did not reduce the expression of genes encoding HD components in HaCaT cells (Figure 1e and f). Expression of the genes involved in cornification (*TGM1*, *PPL*, and *EVPL*) was not affected by the Wnt inhibitor treatments, indicating that the reduction of HD components at the protein level was not due to cell differentiation (Figure 1e and f).

We questioned whether the quantitative changes in HD proteins caused by Wnt inhibitors reflect their localization in the cells and the manifestation of HD-like structures. We observed HD-like structures of HaCaT cells with transmission electron microscopy (Figure 2a and b). In line with the quantitative reduction of HD components by Wnt inhibition (Figure 1a–d), HD-like structures were reduced in Wnt-inhibited HaCaT cells (Figure 2a and b). Because we confirmed that ultrastructural changes were caused by Wnt inhibition, we thereafter focused on PCN as an inner plaque and COL17 as an outer plaque protein of HDs (Hirako and Owaribe, 1998). Immunofluorescence (IF) analysis showed the reduction of PCN and COL17 after Wnt inhibition at the basal side of the HaCaT cells, where HD-like structures were enriched (Figure 2c–h, dashed arrows). These data suggest that Wnt inhibition diminishes HD-like structures in cultured cells at the post-transcriptional level.

Wnt inhibition reduces HD components in vivo

To determine whether these HD proteins are also controlled by Wnt signaling in vivo, we utilized K14-ΔN*Lef1* mice as a model of inactive Wnt signaling in the epidermis (Niemann et al., 2002). These mice express Lef1 that is defective for a β-catenin–binding site under keratin 14 promoter (Niemann et al., 2002). In line with the in vitro data (Figure 2a–h), PCN and COL17 were decreased in the dermo–epidermal junction (DEJ), where HDs are present, in K14-ΔN*Lef1* skin (Figure 3a–d). Thus, these data show that Wnt signaling controls the localization of HD proteins.

PCN deficiency or loss of PCN–COL17 binding phenocopies in Wnt-inhibited cells

Because HD components were comparable in the soluble fraction but were reduced in the HD-rich fraction of the Wnt-inhibited cells (Figure 1a–d and Supplementary Figure S2), we hypothesized that Wnt inhibition leads to HD disassembly, causing the diffusion of HD components into the non-HD plasma membrane. We studied the functions of PCN to confirm this hypothesis further because this protein is a linker between intermediate filaments and HD components to assemble and maintain HDs (Castañón et al., 2013; Natsuga, 2015). We generated PCN-null HaCaT cells (*PLEC* knockout [KO]) using the CRISPR-Cas9 system. COL17 labeling was reduced at the basal side but was more clearly observed at the lateral side of the *PLEC*-KO HaCaT cells than in the control cells (Figure 4a–c, dashed arrows), recapitulating the phenotypes of Wnt-inhibited cells (Figure 2f and h). We also utilized human

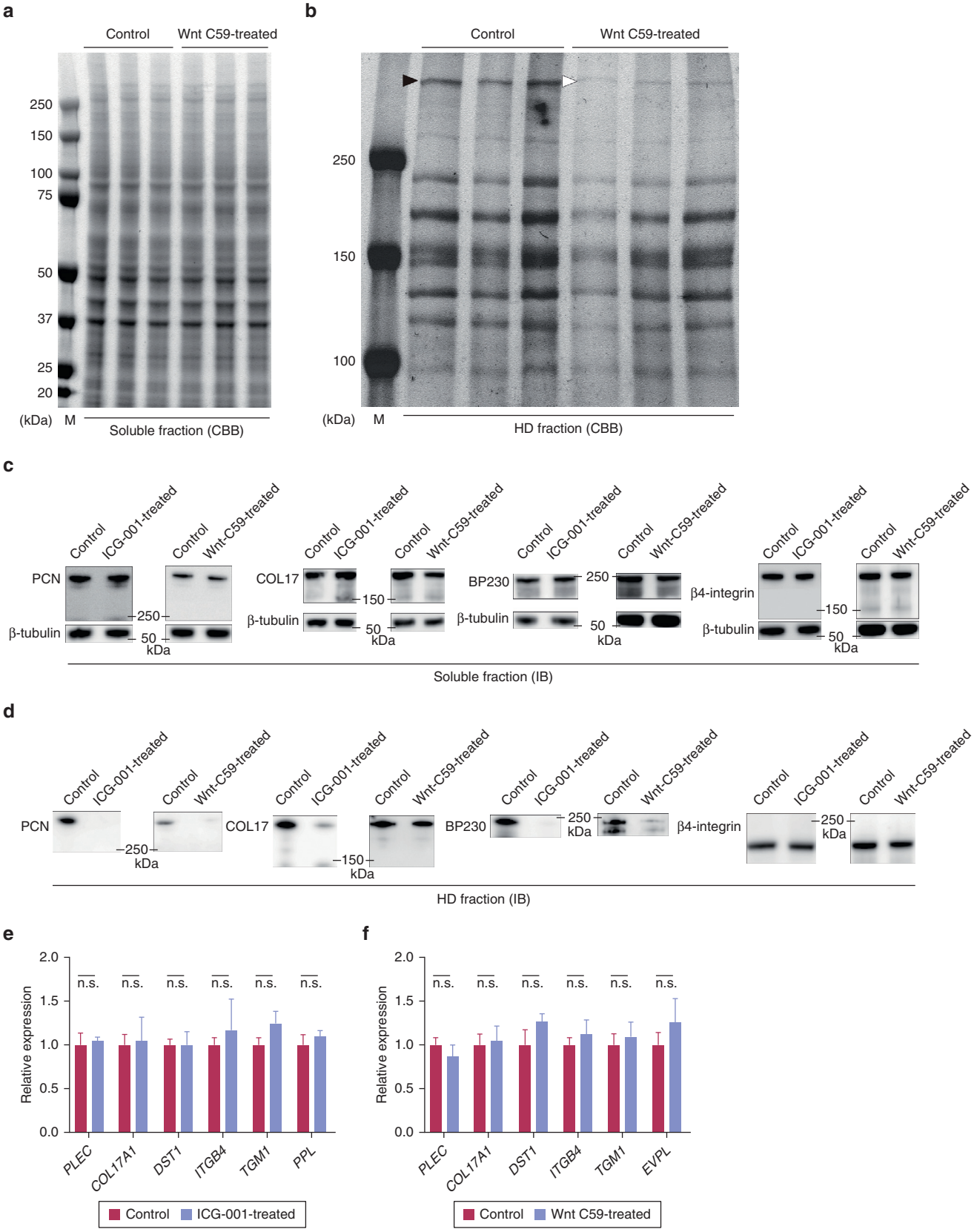

Figure 1. Reduction of HD components identified by screening with Wnt inhibitors. (**a, b**) CBB staining of Wnt C59–treated HaCaT cell (**a**) SFs and (**b**) HDFs. Wnt C59 does not alter SF but reduces the protein above 250 kDa (arrowhead in **b**) in HDF. Plectin is the most likely protein of the band in mass spectrometry. (**c, d**) Immunoblotting of HD proteins in Wnt-inhibited (**c**) SF and (**d**) HDF. (**d**) HD PCN, COL17, and BP230 are reduced in Wnt-inhibited HDF. Representative images are shown from three or more replicates in each group. (**e, f**) RT-qPCR of HD component genes and KC differentiation markers. Wnt inhibition does not affect the expression levels of these genes. n = 3. Student's *t*-test. CBB, coomassie brilliant blue; COL17, type XVII collagen; HD, hemidesmosome; HDF, hemidesmosome-rich fraction; IB, immunoblot; n.s., not significant; PCN, plectin; SF, soluble fraction.

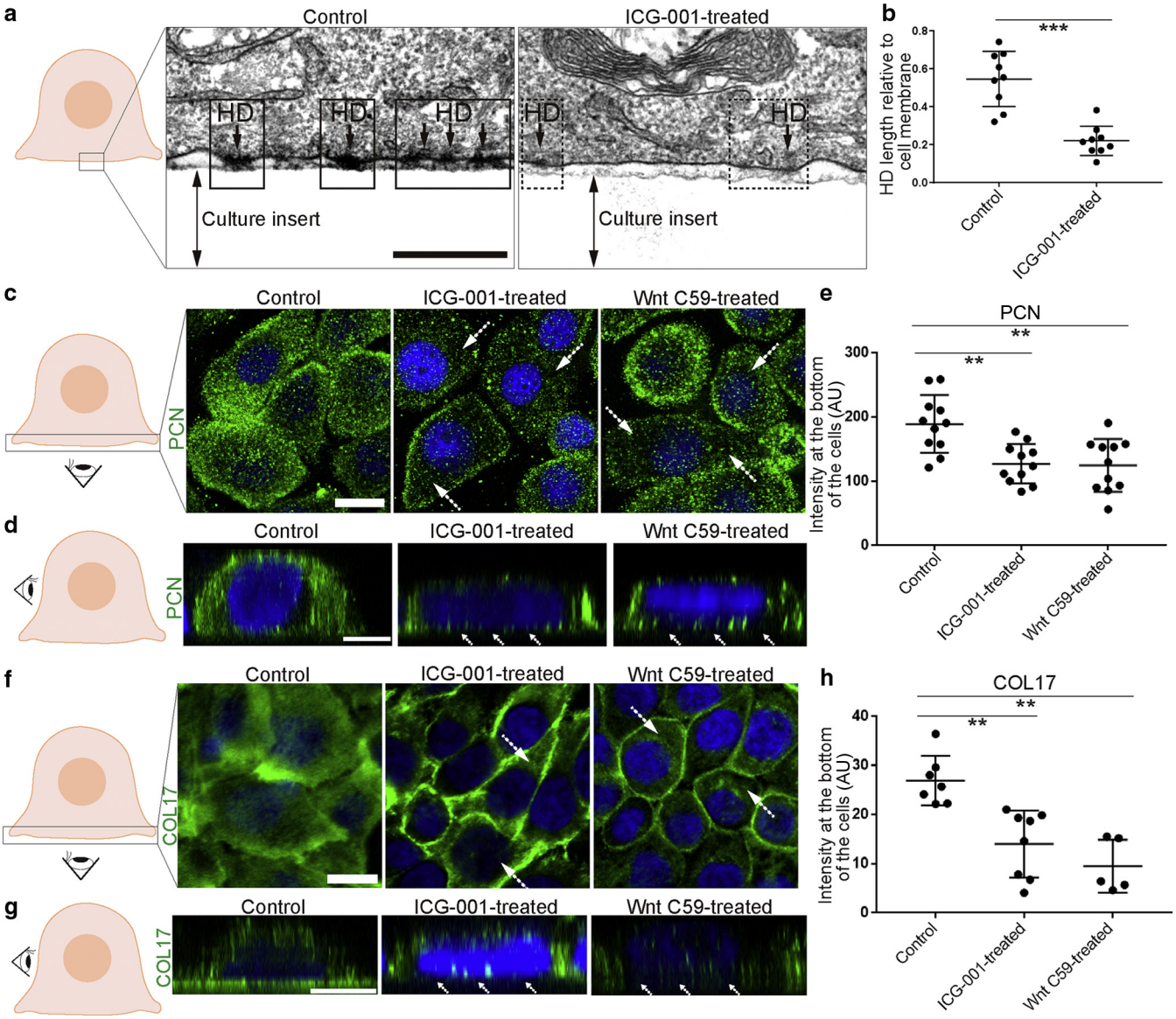

Figure 2. HD reduction of Wnt-inhibited HaCaT cells. (**a**) TEM observation of Wnt-inhibited HaCaT cells. HD-like structures (square) are reduced with Wnt inhibition (dashed square). Bar = 0.5 μm. (**b**) Quantitative analysis of HD-like structures. Mann–Whitney test. (**c**) PCN labeling of Wnt-inhibited HaCaT cells with DAPI counterstain. PCN is partially reduced in the Wnt-inhibited cells (dashed arrows). Bar = 20 μm. (**d**) Optical sectioning of three-dimensional–reconstructed PCN-labeled cells. Bar = 10 μm. (**e**) PCN signal intensity at the basal side of the cells. Dunn's multiple comparison test. (**f**) COL17 labeling of Wnt-inhibited HaCaT cells. Bar = 20 μm. (**g**) Optical sectioning of three-dimensional–reconstructed COL17-labeled cells. (**h**) COL17 signal intensity at the basal side of the cells. Bar = 10 μm. Dunn's multiple comparison test. **$0.001 < P < 0.01$, ***$0.0001 < P < 0.001$. AU, arbitrary unit; COL17, type XVII collagen; HD, hemidesmosome; PCN, plectin; TEM, transmission electron microscope.

epidermal KCs derived from patients with EB simplex with defective PCN–COL17 binding due to *PLEC* compound heterozygous sequence variants, including that of the COL17-binding region (Natsuga et al., 2017). Defective PCN–COL17 binding led to COL17 distribution at the lateral side rather than at the basal side of the cells (Figure 4d–f, dashed arrows), as was seen in *PLEC*-KO and Wnt-inhibited HaCaT cells. This staining pattern in the cultured cells was also compatible with that in the patient's skin, which showed a reduction in both PCN and COL17 at the DEJ (Natsuga et al., 2017). These data imply that Wnt/β-catenin signaling might be involved in HD assembly.

Atypical protein kinase C inhibition alleviates the Wnt-inhibited phenotypes

We then hypothesized that the modulation of HD components by Wnt inhibition is mediated through the protein kinase C (PKC) pathway because activated PKC interacts with PCN and translocates PCN into the cytoskeleton in mouse fibroblasts (Osmanagic-Myers and Wiche, 2004). In addition, COL17 phosphorylation by PKC changes the distribution of COL17 in cultured KCs (Iwata et al., 2016). To test this hypothesis, we treated HaCaT cells with Go6983, a pan-PKC inhibitor, and found that the reduction in PCN and COL17 levels through Wnt inhibition was ameliorated by

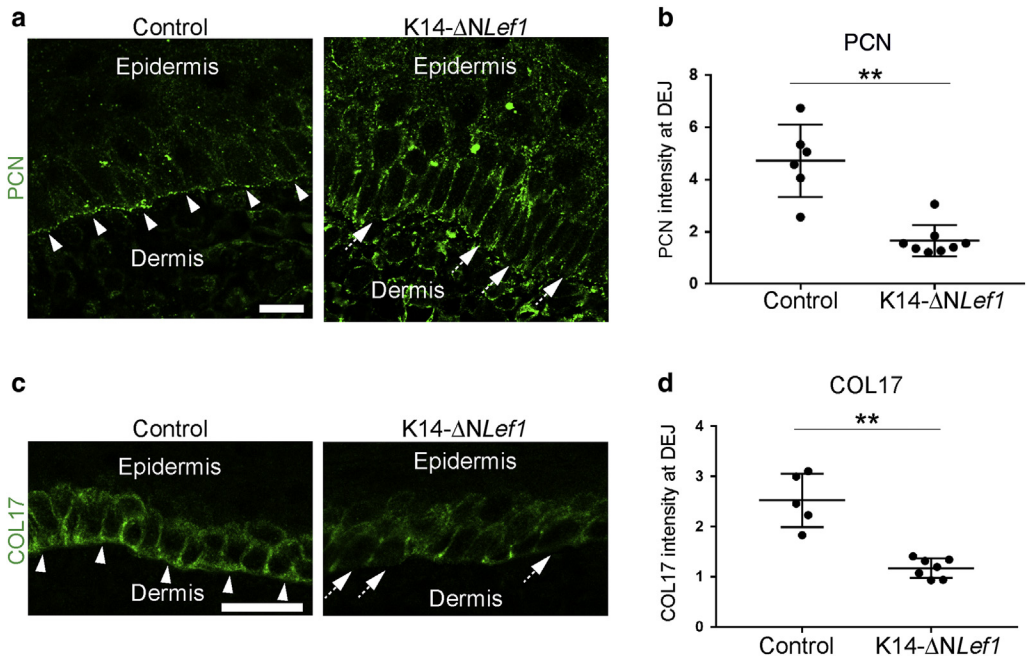

Figure 3. PCN and COL17 reduction at the DEJ of Wnt-inactive epidermis. (**a**) PCN labeling of K14-ΔN*Lef1* epidermis. (**b**) PCN signal intensity at the DEJ where HDs are present. (**c**) COL17 labeling of K14-ΔN*lef1* epidermis. (**d**) COL17 signal intensity at the DEJ. The signal intensity is normalized to that of the basal KCs at the lateral cell periphery (**b, d**). PCN and COL17 (arrows in **a** and **c**) are reduced at the DEJ of K14-ΔN*Lef1* mice (dashed arrows in **a** and **c**). Bar = 20 μm. Mann–Whitney test. **0.001 < P < 0.01. COL17, type XVII collagen; DEJ, dermo–epidermal junction; HD, hemidesmosome; K14, keratin 14; PCN, plectin.

PKC inhibitor treatment (Figure 5a–f). To clarify which subtype of PKC mediates Wnt-induced HD disarrangement, we performed specific PKC inhibitor treatment for Wnt-inhibited HaCaT cells. We utilized CRT0066854 as an atypical PKC (aPKC) (PKC ζ, ι/λ) inhibitor (Kjær et al., 2013) and GF109203X as a classical (PKC α, β, γ) and novel PKC (PKC δ, ε, η, θ) inhibitor (Toullec et al., 1991). We found that whereas aPKC inhibition rescues the phenotype of Wnt inhibition in HaCaT cells, classical/novel PKC inhibition does not (Figure 6a–f). These data suggest that aPKC mediates Wnt inhibition–induced HD disarrangement.

DISCUSSION

Although Wnt/β-catenin signaling is fundamental for skin development and homeostasis (Lim and Nusse, 2013), whether and how Wnt/β-catenin signaling affects HD proteins is unknown. In this study, we uncovered the role of Wnt/β-catenin signaling in the spatial regulation of HD components (Figure 6g). Inhibition of Wnt/β-catenin signaling reduces HD PCN and COL17 in both in vitro and in vivo settings. *PLEC* KO or disturbed PCN–COL17 interaction reproduces the HD-less phenotype of Wnt-inactive cells. aPKC inhibition ameliorates HD disarrangement in Wnt-inactive cells.

Previous reports have revealed that HD components such as COL17 and PCN could be upstream modulators of Wnt signaling (Sorial et al., 2020; Watanabe et al., 2017; Yin et al., 2021). Our group previously reported that COL17, an HD protein, is a Wnt stabilizer in the epidermis (Watanabe et al., 2017). During skeletal muscle development, PCN plays a vital role in promoting myoblast differentiation and proliferation by binding to dishevelled-2 and forming a protein complex, which subsequently activates canonical Wnt signaling (Yin et al., 2021). Moreover, knockdown of *PLEC* in cartilage and synovium cells resulted in decreased Wnt-related genes in the transcriptomic analysis (Sorial et al., 2020). Our study suggests that HD components such as COL17 and PCN can be not only upstream modulators of Wnt signaling but also target proteins of Wnt/β-catenin signaling.

Our study shows that Wnt-induced reduction of HD components at the basal side of the cells is mediated by aPKC. aPKC is a cell polarity regulator that forms a complex with partitioning-defective (PAR) proteins (Suzuki and Ohno, 2006). COL17 interacts with the aPKC–PAR complex and contributes to maintaining epidermal cell polarity (Liu et al., 2019; Matsumura et al., 2021; Watanabe et al., 2021). Pharmacological aPKC inhibition of three-dimensional–reconstituted epidermis reduces nonhemidesmosomal COL17 at the lateral portions of KCs while maintaining hemidesmosomal COL17 (Watanabe et al., 2017). These previous findings are compatible with our data.

EB is a group of genetic dermatoses characterized by mucocutaneous fragility and blister formation (Has et al., 2020a). Missing or dysfunctional DEJ molecules weaken epidermal–dermal adhesion, resulting in blisters with minimal mechanical trauma (Has et al., 2020b). Although various therapeutic modalities have been developed for EB (Has et al., 2020b), there has been no strategy to strengthen epidermal–dermal adhesion without gene modulation or protein replacement. Our findings that the Wnt signaling pathway modulates HDs could be extrapolated into EB treatment because stable HDs might augment epidermal attachment to the dermis even when one of the DEJ components is dysfunctional. Recently, pharmacological Wnt modulation by suppressing Wnt-inhibitive molecules has been proposed to remedy hair loss disorders (Hawkshaw et al., 2018). This approach can be applied to EB as disease-modifying therapy.

In conclusion, our study revealed an unrecognized link between Wnt/β-catenin signaling and HDs in KCs. We

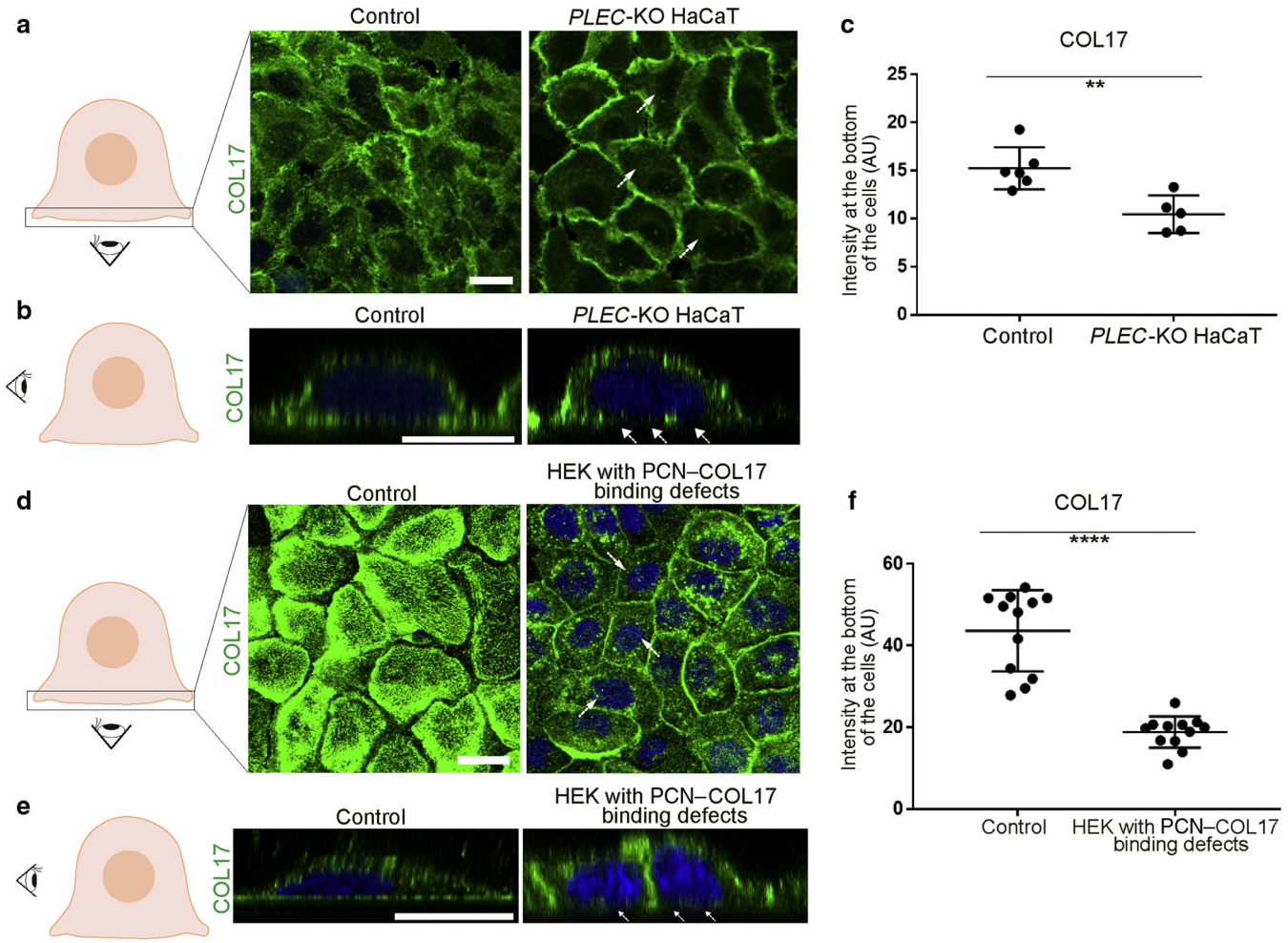

Figure 4. COL17 reduction at the basal side of PCN-null HaCaT cells or EB keratinocytes with defective PCN–COL17 binding. (**a**) COL17 labeling of *PLEC*-KO HaCaT cells with DAPI counterstain. Images are obtained at the basal side of the cells. (**b**) Optical sectioning of 3D-reconstructed *PLEC*-KO HaCaT cells. COL17 is reduced at the basal side of the cells (dashed arrows). Bar = 10 μm. (**c**) COL17 signal intensity at the basal side of the cells. (**d**) COL17 labeling of EB keratinocytes with PCN–COL17 binding defects. (**e**) Optical sectioning of 3D-reconstructed cells. COL17 is reduced at the basal side of the EB keratinocytes (dashed arrows). (**f**) COL17 signal intensity at the basal side of the cells. Bar = 10 μm. Mann–Whitney test. $^{**}0.001 < P < 0.01$, $^{****}P < 0.0001$. 3D, three-dimensional; AU, arbitrary unit; COL17, type XVII collagen; EB, epidermolysis bullosa; HEK, human epidermal keratinocyte; KO, knockout; PCN, plectin.

propose that Wnt/aPKC-modulating molecules could be therapeutic candidates for EB.

MATERIALS AND METHODS

Ethics

For animal experimentation, the Institutional Review Board of the Hokkaido University Graduate School of Medicine (Sapporo, Japan) approved all animal studies described in the following sections. The Institutional Review Board of the Hokkaido University Graduate School of Medicine approved all human studies described in the following sections (identification 13-043). The study was conducted in accordance with the principles of the Declaration of Helsinki. The participants' legal representatives provided written informed consent.

Antibodies

The following antibodies were used: anti-nonphosphorylated β-catenin (Ser33/37/Thr41) (Cell Signaling Technology, Danvers, MA), anti-tubulin (Abcam, Cambridge, United Kingdom), anti-PCN *N*-terminal region (PN643) (Natsuga et al., 2010), anti-PCN *C*-terminal region (Abcam), anti-COL17 C-terminal region (09040) (Ujiie et al., 2014), anti-COL17 cytoplasmic region (Abcam), anti-integrin β4 (Santa Cruz Biotechnology, Dallas, TX), and anti-BP230 (S1196) (kindly provided by John Stanley).

Cell line

HaCaT cells (CLS Cell Lines Service, Eppelheim, Germany) and NHEKs (Lonza, Basel, Switzerland) were used for the analysis. EB simplex KCs were obtained from a patient who was compound heterozygous for truncation and in-frame deletion variants in *PLEC*. The latter variant (c.2264_2266del/p.Phe775del) hinders COL17 binding to PCN (Natsuga et al., 2017). EB simplex KCs were immortalized with Lenti-X 293T cells (Takara Bio, Kusatsu, Japan) transfected with the HPV16 E6/E7-containing vector and lentiviral high-titer packaging mixture (Takara Bio) according to the manufacturer's instructions. The supernatants were collected and added to the proband's cultured KCs, together with polybrene (Sigma-Aldrich, St. Louis, MO). Immortalized cells were selected with puromycin (Life Technologies, Carlsbad, CA) and used for IF. HaCaT cells, immortalized KCs from the patient with EB simplex,

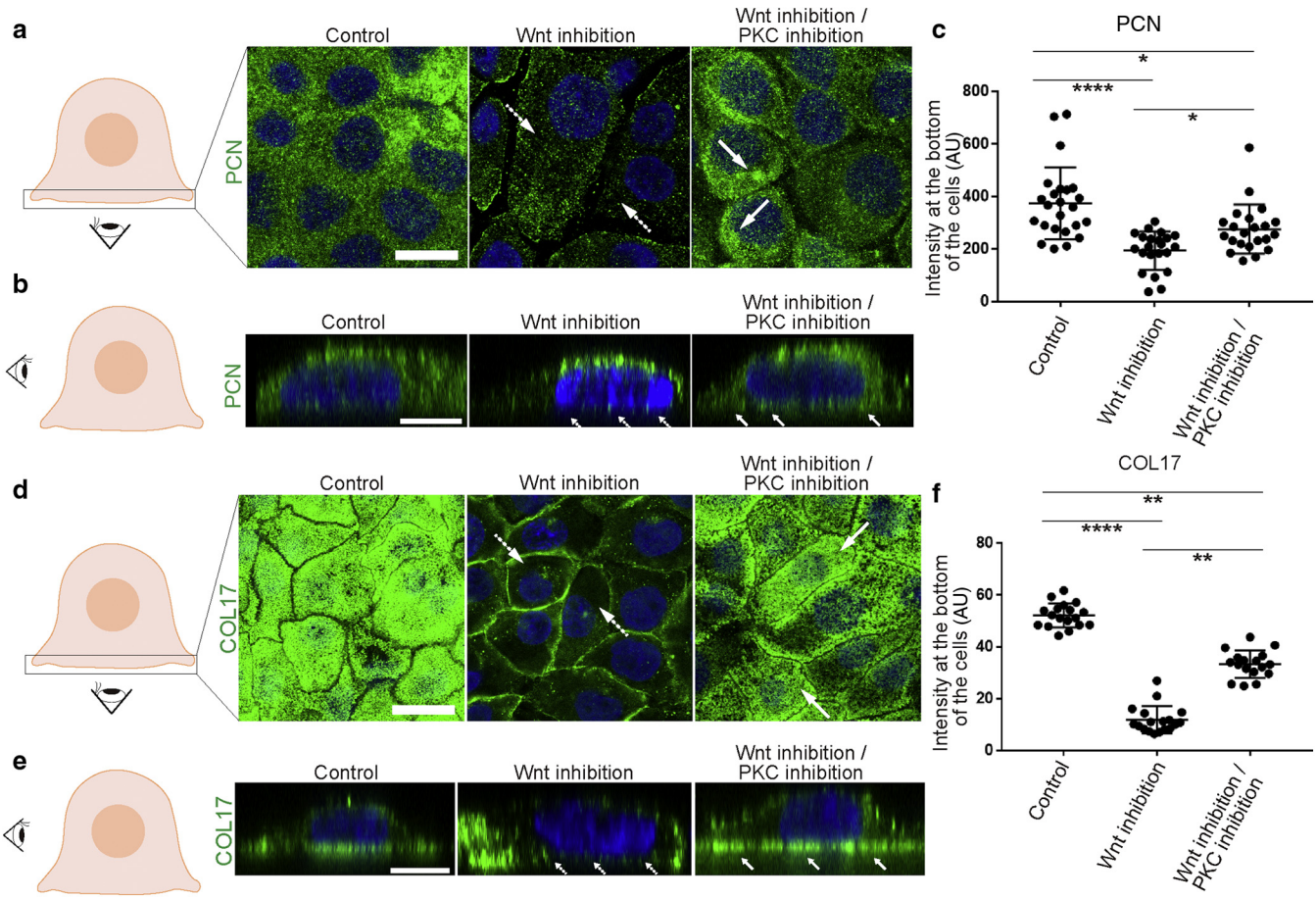

Figure 5. Partial rescue of Wnt-inhibited phenotypes by PKC inhibition. (**a**) PCN labeling of HaCaT cells treated with Wnt inhibitor (ICG-001) with or without PKC inhibitor (Go6983). Images are obtained at the basal side of the cells. Bar = 20 μm. Counterstain: DAPI. (**b**) Optical sectioning of 3D-reconstructed plectin-labeled cells (Bar = 10 μm). PCN is diminished in Wnt-inhibited cells (dashed arrows) and is partially rescued with PKC inhibition (arrows). (**c**) PCN signal intensity at the bottom of the cells. (**d**) COL17 labeling of HaCaT cells treated with Wnt and/or PKC inhibitors. Bar = 20 μm. (**e**) Optical sectioning of 3D-reconstructed COL17-labeled cells (Bar = 10 μm). (**f**) COL17 signal intensity at the bottom of the cells. Dunn's multiple comparison test. *$0.01 < P < 0.05$, **$0.001 < P < 0.01$, ****$P < 0.0001$. 3D, three-dimensional; AU, arbitrary unit; COL17, type XVII collagen; PCN, plectin; PKC, protein kinase C.

and NHEKs were cultured in a serum-free KC growth medium (Lonza).

IF study of cultured cells

Cultured cells were fixed with 4% paraformaldehyde, followed by permeabilization with 0.1% Triton X-100 in PBS for 20 minutes at room temperature. The cells were then incubated with primary antibodies overnight at 4 °C. After washing in PBS, the cells were incubated with secondary antibodies conjugated with Alexa488 or Alexa647 for 1 hour at room temperature. The nuclei were stained with DAPI. All stained immunofluorescent samples were observed using a confocal laser scanning microscope (LSM710, Carl Zeiss, Oberkochen, Germany) and analyzed using Zeiss LSM710 software. Z-stack images were taken using multiple z-planes (0.5-μm intervals). The signal intensity at the basal side of the cells facing the dish was quantified using ImageJ software (National Institutes of Health, Bethesda, MD) and normalized to the area used for quantification.

Electron microscopy

HaCaT cells were cultured in KC growth medium on cell culture inserts (Greiner Bio-One ThinCert [0.4μm pore], Greiner Bio-One, Kremsmunster, Germany). Before cell culturing, the inserts were coated with CELLstart (Thermo Fisher Scientific, Waltham, MA). HaCaT cells on the inserts were fixed with 2% glutaraldehyde/2% paraformaldehyde in 30 mM 4-(2-hydroxyethyl)-1-piperazineethanesulfonic acid buffer. The samples were dehydrated and embedded in Epon 812. Thin-sections for electron microscopy were cut to 70 nm thickness, stained with uranyl acetate and lead citrate, and examined using JEM1400 (Japan Electron Optics Laboratory, Tokyo, Japan). The total length of HD-like structures along the cell membrane was measured using ImageJ software and normalized using the cell membrane length at the basal side of the cell.

Animals and IF intensity analysis

Specimens from K14-Δ*N*Lef1 (RRID:MGI:2667413) (Niemann et al., 2002) mice paw skin at postnatal day 1 were fixed with formalin and embedded in paraffin after dehydration. Antigen retrieval with pH 6.0 citrate buffer was performed on deparaffinized sections. Sections were incubated with primary antibodies overnight at 4 °C. After washing in PBS, the sections were incubated with secondary antibodies conjugated with Alexa488 for 1 hour at room temperature. The fluorescent signal intensity at the DEJ was quantified using ZEN software (Carl Zeiss) and normalized to the signal intensity at the lateral cellular periphery.

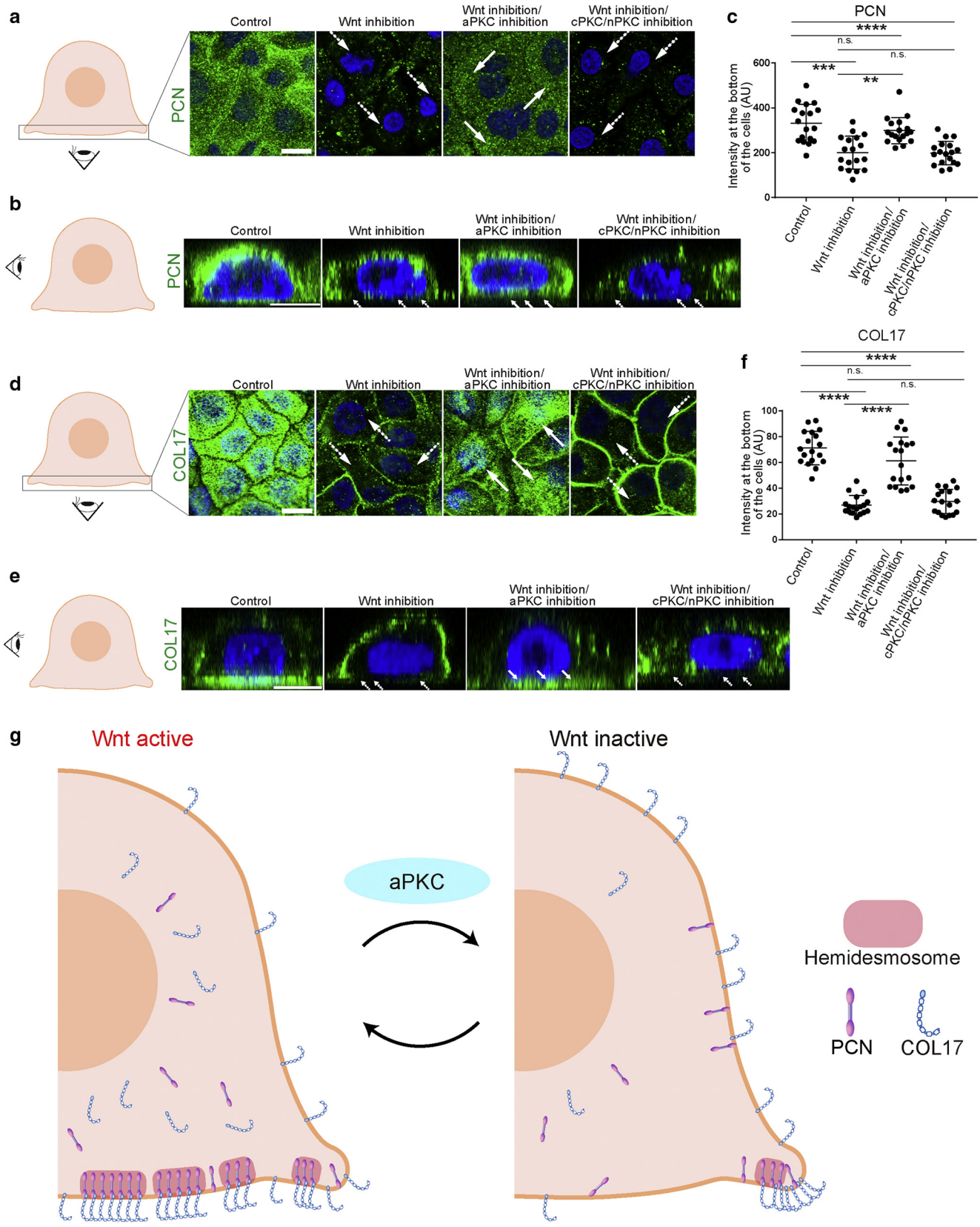

Figure 6. Alleviation of the Wnt-inhibited phenotypes by aPKC inhibition. (**a**–**f**) aPKC inhibitor (CRT0066854) or cPKC/nPKC inhibitor (GF109203X) are applied to Wnt-inhibited HaCaT cells. (**a**) PCN staining of HaCaT cells. Images are obtained at the basal side of the cells facing the dish with DAPI counterstain. Bar = 20 μm. (**b**) Optical sectioning of 3D-reconstructed PCN-labeled cells (Bar = 10 μm). (**c**) PCN signal intensity at the bottom of the cells. (**d**) COL17 labeling of HaCaT cells. Bar = 20 μm. (**e**) Optical sectioning of 3D-reconstructed COL17-labeled cells (Bar = 10 μm). (**f**) COL17 signal intensity at the bottom of the cells. Dunn's multiple comparison test. $^{**}0.001 < P < 0.01$, $^{***}0.0001 < P < 0.001$, $^{****}P < 0.0001$. (**g**) Graphical abstract of this study. 3D, three-dimensional; aPKC, atypical protein kinase C; AU, arbitrary unit; COL17, type XVII collagen; cPKC, classical protein kinase C; n.s., not significant; nPKC, novel protein kinase C; PCN, plectin; PKC, protein kinase C.

Isolation of the whole-cell lysate, soluble fractions, and HD-rich fractions from HaCaT and NHEKs

Cultured cells were grown to 90–100% confluence with KC growth medium as described earlier. For whole-cell lysate extraction, cells were lysed in a 2% SDS-containing buffer. The supernatant was collected after centrifugation. For soluble fraction extraction, cells were collected and lysed in 1% NP-40–containing buffer. To extract the HD-rich fraction, the cells were treated with 20 mM ammonia hydroxide, followed by 0.1% Triton X-100 in PBS. HD-rich fractions were solubilized in a 2% SDS buffer (Hirako et al., 2014). The protein concentration of each HD-rich lysate was calculated using the QuickStart Bradford Protein Assay (Bio-Rad Laboratories, Richmond, CA), and the lysates were subsequently equalized before SDS-PAGE. All lysates were treated with 5% 2-mercaptoethanol and boiled before immunoblotting analysis.

Immunoblotting analysis

Lysate samples were applied to 4–10% NuPAGE gradient gel (Invitrogen, Carlsbad, CA), 4–13% gradient polyacrylamide gel, or 7% polyacrylamide gel. The gels were stained with coomassie brilliant blue or transferred to polyvinylidene fluoride membranes for subsequent immunoblotting. The membranes were incubated with primary antibodies, followed by incubation with horseradish peroxidase–conjugated anti-mouse IgG or horseradish peroxidase–conjugated anti-rabbit IgG. The blots were detected using an ECL Plus Detection Kit (GE Healthcare, Fairfield, CT). Images were obtained using a LAS-4000 mini (Fujifilm, Tokyo, Japan). The relative ratio of the band intensity of active β-catenin to β-tubulin was quantified using ImageJ software.

Protein identification by mass spectrometry

Mass spectrometric analysis was performed using a combination of Fourier transform mass spectrometry and ion trap tandem mass spectrometry. Briefly, the HD-rich fraction was subjected to SDS-PAGE. The band of interest was manually excised from the gel stained with SimplyBlue SafeStain (Invitrogen, Carlsbad, CA). The gel piece was washed three times with 50% acetonitrile in 25 mM ammonium bicarbonate, hydrated with 100% acetonitrile, and dried in a vacuum evaporator. The gel pieces were digested with 20 ng/ml trypsin solution at 37 °C overnight. The resultant peptide mixtures were extracted twice with 0.1% trifluoroacetic acid/50% acetonitrile. The extracted peptides were concentrated in a centrifugal vacuum evaporator and subjected to mass spectrometric analysis.

RT-qPCR

The RNA solution was extracted from cultured HaCaT cells and NHEKs using the RNeasy Mini kit (Qiagen, Hilden, Germany), and cDNA was prepared using the SuperScript III First-Strand Synthesis System (Thermo Fisher Scientific). RT-qPCR was performed using the designated primers and fast SYBR Green (Thermo Fisher Scientific) in a STEP-One plus sequence detection system (Applied Biosystems, Waltham, MA). All primers used in this study are listed in Supplementary Table S1. The housekeeping gene *YWHAZ* was used to compare NHEK with HaCaT cells and *18S* was used as a housekeeping gene.

Chemical treatment of cultured cells

In Wnt-inhibition treatment, either Wnt C59 or ICG-001 (Cayman Chemical, Ann Arbor, MI) dissolved in DMSO was added to the culture medium 48 hours before lysate preparation, RNA extraction, IF or electron microscopy analysis (Emami et al., 2004; Proffitt et al., 2013). Unless specified, Wnt C59 and ICG-001 were used at final concentrations of 5 μM and 10 μM, respectively. In PKC inhibition, Go6983 (Tocris Bio, Bristol, United Kingdom), CRT0066854 (Axon Medchem, Groningen, The Netherlands), and GF109203X (Merck, Darmstadt, Germany) were applied to cells 48 hours before IF analysis. Go6983, CRT0066854, and GF109203X were used at final concentrations of 20 μM, 639 nM, and 0.21 μM, respectively. Wnt3a-conditioned medium was added to the dish at a final concentration of 30% of the total medium by volume 24 hours before lysate extraction.

CRISPR/Cas9-mediated gene editing in HaCaT cells

To perform CRISPR/Cas9-mediated gene editing in HaCaT cells, Cas9 nuclease- and guide RNA–expressing vectors were transfected into HaCaT cells, as reported previously (Shinkuma et al., 2016; Takashima et al., 2019). The guide RNA was designed to target exon 19 (targeting GGGGCAGTTGCAGAAGCTGC) of the *PLEC* gene (NM_000445.4). After sorting by flow cytometry and single-cell selection, direct sequencing analysis was performed. HaCaT cells with a homozygous deletion variant in *PLEC* (c.2303del) were used for further analysis. IF, immunoblotting, and RT-qPCR analyses confirmed *PLEC KO* KO in the cells.

Statistical analysis

Statistical analysis was performed using GraphPad Prism (GraphPad Software, San Diego, CA). *P*-values were determined using Student's *t*-test, Mann–Whitney test, or Dunn's multiple comparison test. *P*-values were indicated as $*0.01 < P < 0.05$, $**0.001 < P < 0.01$, $***0.0001 < P < 0.001$, and $****P < 0.0001$.

Data availability statement

No datasets were generated or analyzed during this study.

ORCIDs

Hideyuki Kosumi: http://orcid.org/0000-0003-2955-6486
Mika Watanabe: http://orcid.org/0000-0002-0075-0851
Satoru Shinkuma: http://orcid.org/0000-0002-6429-1498
Takuma Nohara: http://orcid.org/0000-0001-9842-4394
Yu Fujimura: http://orcid.org/0000-0003-0534-5561
Tadasuke Tsukiyama: http://orcid.org/0000-0001-5205-8202
Giacomo Donati: http://orcid.org/0000-0002-0370-8288
Hiroaki Iwata: http://orcid.org/0000-0002-8781-2735
Hideki Nakamura: http://orcid.org/0000-0002-9132-9260
Hideyuki Ujiie: http://orcid.org/0000-0002-3489-5418
Ken Natsuga: http://orcid.org/0000-0003-3865-6366

CONFLICT OF INTEREST

The authors state no conflict of interest.

ACKNOWLEDGMENTS

We thank the Global Facility Center, Hokkaido University for allowing us to conduct mass spectrometric analysis. We also thank Fiona M. Watt for providing K14-ΔN*Lef1* mice and Shinji Takeda for the Wnt3a-conditioned medium. This work was funded by Japan Agency for Medical Research and Development (identification 20ek0109380h0003).

AUTHOR CONTRIBUTIONS

Conceptualization: HK, KN; Funding Acquisition: KN; Investigation: HK, MW, SS, TN, YF, TT, GD, HI, HN; Supervision: HU, KN; Writing - Original Draft Preparation: HK, KN; Writing - Review and Editing: HK, KN

SUPPLEMENTARY MATERIAL

Supplementary material is linked to the online version of the paper at www.jidonline.org, and at https://doi.org/10.1016/j.jid.2021.10.018.

REFERENCES

Andrä K, Lassmann H, Bittner R, Shorny S, Fässler R, Propst F, et al. Targeted inactivation of plectin reveals essential function in maintaining the integrity of skin, muscle, and heart cytoarchitecture. Genes Dev 1997;11:3143–56.

Borradori L, Sonnenberg A. Structure and function of hemidesmosomes: more than simple adhesion complexes. J Invest Dermatol 1999;112:411–8.

Bryja V, Schulte G, Arenas E. Wnt-3a utilizes a novel low dose and rapid pathway that does not require casein kinase 1-mediated phosphorylation of Dvl to activate beta-catenin. Cell Signal 2007;19:610–6.

Castañón MJ, Walko G, Winter L, Wiche G. Plectin-intermediate filament partnership in skin, skeletal muscle, and peripheral nerve. Histochem Cell Biol 2013;140:33–53.

Chetty BV, Boissy RE, Warden GD, Nordlund JJ. Basement membrane and fibroblast aberration in blisters at the donor, graft, and spontaneously healed sites in patients with burns. Arch Dermatol 1992;128:181–6.

Dowling J, Yu QC, Fuchs E. Beta4 integrin is required for hemidesmosome formation, cell adhesion and cell survival. J Cell Biol 1996;134:559–72.

Emami KH, Nguyen C, Ma H, Kim DH, Jeong KW, Eguchi M, et al. A small molecule inhibitor of beta-catenin/CREB-binding protein transcription [corrected] [published correction appears in Proc Natl Acad Sci USA 2004;101:16707]. Proc Natl Acad Sci USA 2004;101:12682–7.

Fontao L, Tasanen K, Huber M, Hohl D, Koster J, Bruckner-Tuderman L, et al. Molecular consequences of deletion of the cytoplasmic domain of bullous pemphigoid 180 in a patient with predominant features of epidermolysis bullosa simplex. J Invest Dermatol 2004;122:65–72.

Frijns E, Kuikman I, Litjens S, Raspe M, Jalink K, Ports M, et al. Phosphorylation of threonine 1736 in the C-terminal tail of integrin β4 contributes to hemidesmosome disassembly. Mol Biol Cell 2012;23:1475–85.

Frijns E, Sachs N, Kreft M, Wilhelmsen K, Sonnenberg A. EGF-induced MAPK signaling inhibits hemidesmosome formation through phosphorylation of the integrin {beta}4. J Biol Chem 2010;285:37650–62.

Fujimura Y, Watanabe M, Ohno K, Kobayashi Y, Takashima S, Nakamura H, et al. Hair follicle stem cell progeny heal blisters while pausing skin development. EMBO Rep 2021;22:e50882.

Geerts D, Fontao L, Nievers MG, Schaapveld RQ, Purkis PE, Wheeler GN, et al. Binding of integrin alpha6beta4 to plectin prevents plectin association with F-actin but does not interfere with intermediate filament binding. J Cell Biol 1999;147:417–34.

Georges-Labouesse E, Messaddeq N, Yehia G, Cadalbert L, Dierich A, Le Meur M. Absence of integrin alpha 6 leads to epidermolysis bullosa and neonatal death in mice. Nat Genet 1996;13:370–3.

Has C, Bauer JW, Bodemer C, Bolling MC, Bruckner-Tuderman L, Diem A, et al. Consensus reclassification of inherited epidermolysis bullosa and other disorders with skin fragility. Br J Dermatol 2020a;183:614–27.

Has C, South A, Uitto J. Molecular therapeutics in development for epidermolysis bullosa: update 2020. Mol Diagn Ther 2020b;24:299–309.

Hawkshaw NJ, Hardman JA, Haslam IS, Shahmalak A, Gilhar A, Lim X, et al. Identifying novel strategies for treating human hair loss disorders: cyclosporine A suppresses the Wnt inhibitor, SFRP1, in the dermal papilla of human scalp hair follicles. PLoS Biol 2018;16:e2003705.

Hirako Y, Owaribe K. Hemidesmosomes and their unique transmembrane protein BP180. Microsc Res Tech 1998;43:207–17.

Hirako Y, Yonemoto Y, Yamauchi T, Nishizawa Y, Kawamoto Y, Owaribe K. Isolation of a hemidesmosome-rich fraction from a human squamous cell carcinoma cell line. Exp Cell Res 2014;324:172–82.

Iwata H, Kamaguchi M, Ujiie H, Nishimura M, Izumi K, Natsuga K, et al. Macropinocytosis of type XVII collagen induced by bullous pemphigoid IgG is regulated via protein kinase C. Lab Invest 2016;96:1301–10.

Kiistala U, Mustakallio KK. Dermo-epidermal separation with suction. Electron microscopic and histochemical study of initial events of blistering on human skin. J Invest Dermatol 1967;48:466–77.

Kjær S, Linch M, Purkiss A, Kostelecky B, Knowles PP, Rosse C, et al. Adenosine-binding motif mimicry and cellular effects of a thieno[2,3-d] pyrimidine-based chemical inhibitor of atypical protein kinase C isoenzymes. Biochem J 2013;451:329–42.

Koster J, Geerts D, Favre B, Borradori L, Sonnenberg A. Analysis of the interactions between BP180, BP230, plectin and the integrin alpha6-beta4 important for hemidesmosome assembly. J Cell Sci 2003;116:387–99.

Koster J, Kuikman I, Kreft M, Sonnenberg A. Two different mutations in the cytoplasmic domain of the integrin beta 4 subunit in nonlethal forms of epidermolysis bullosa prevent interaction of beta 4 with plectin [published correction appears in J Invest Dermatol 2002;118:910]. J Invest Dermatol 2001;117:1405–11.

Krawczyk WS. A pattern of epidermal cell migration during wound healing. J Cell Biol 1971;49:247–63.

Lien WH, Polak L, Lin M, Lay K, Zheng D, Fuchs E. In vivo transcriptional governance of hair follicle stem cells by canonical Wnt regulators. Nat Cell Biol 2014;16:179–90.

Lim X, Nusse R. Wnt signaling in skin development, homeostasis, and disease. Cold Spring Harb Perspect Biol 2013;5:a008029.

Litjens SH, de Pereda JM, Sonnenberg A. Current insights into the formation and breakdown of hemidesmosomes. Trends Cell Biol 2006;16:376–83.

Liu N, Matsumura H, Kato T, Ichinose S, Takada A, Namiki T, et al. Stem cell competition orchestrates skin homeostasis and ageing. Nature 2019;568:344–50.

Lu C, Fuchs E. Sweat gland progenitors in development, homeostasis, and wound repair. Cold Spring Harb Perspect Med 2014;4:a015222.

Matsumura H, Liu N, Nanba D, Ichinose S, Takada A, Kurata S, et al. Distinct types of stem cell divisions determine organ regeneration and aging in hair follicles. Nat Aging 2021;1:190–204.

Nakano A, Pulkkinen L, Murrell D, Rico J, Lucky AW, Garzon M, et al. Epidermolysis bullosa with congenital pyloric atresia: novel mutations in the beta 4 integrin gene (ITGB4) and genotype/phenotype correlations. Pediatr Res 2001;49:618–26.

Natsuga K. Plectin-related skin diseases. J Dermatol Sci 2015;77:139–45.

Natsuga K, Nishie W, Akiyama M, Nakamura H, Shinkuma S, McMillan JR, et al. Plectin expression patterns determine two distinct subtypes of epidermolysis bullosa simplex. Hum Mutat 2010;31:308–16.

Natsuga K, Nishie W, Nishimura M, Shinkuma S, Watanabe M, Izumi K, et al. Loss of interaction between plectin and type XVII collagen results in epidermolysis bullosa simplex. Hum Mutat 2017;38:1666–70.

Natsuga K, Watanabe M, Nishie W, Shimizu H. Life before and beyond blistering: the role of collagen XVII in epidermal physiology. Exp Dermatol 2019;28:1135–41.

Niemann C, Owens DM, Hülsken J, Birchmeier W, Watt FM. Expression of DeltaNLef1 in mouse epidermis results in differentiation of hair follicles into squamous epidermal cysts and formation of skin tumours. Development 2002;129:95–109.

Nishie W, Sawamura D, Goto M, Ito K, Shibaki A, McMillan JR, et al. Humanization of autoantigen. Nat Med 2007;13:378–83.

Osmanagic-Myers S, Wiche G. PlectinRACK1 (receptor for activated C kinase 1) scaffolding: a novel mechanism to regulate protein kinase C activity. J Biol Chem 2004;279:18701–10.

Proffitt KD, Madan B, Ke Z, Pendharkar V, Ding L, Lee MA, et al. Pharmacological inhibition of the Wnt acyltransferase PORCN prevents growth of WNT-driven mammary cancer. Cancer Res 2013;73:502–7.

Raymond K, Kreft M, Janssen H, Calafat J, Sonnenberg A. Keratinocytes display normal proliferation, survival and differentiation in conditional beta4-integrin knockout mice. J Cell Sci 2005;118:1045–60.

Shinkuma S, Guo Z, Christiano AM. Site-specific genome editing for correction of induced pluripotent stem cells derived from dominant dystrophic epidermolysis bullosa. Proc Natl Acad Sci USA 2016;113:5676–81.

Sorial AK, Hofer IMJ, Tselepi M, Cheung K, Parker E, Deehan DJ, et al. Multi-tissue epigenetic analysis of the osteoarthritis susceptibility locus mapping to the plectin gene PLEC. Osteoarthritis Cartilage 2020;28:1448–58.

Suzuki A, Ohno S. The PAR-aPKC system: lessons in polarity. J Cell Sci 2006;119:979–87.

Takashima S, Shinkuma S, Fujita Y, Nomura T, Ujiie H, Natsuga K, et al. Efficient gene reframing therapy for recessive dystrophic epidermolysis bullosa with CRISPR/Cas9. J Invest Dermatol 2019;139:1711–21.e4.

Toullec D, Pianetti P, Coste H, Bellevergue P, Grand-Perret T, Ajakane M, et al. The bisindolylmaleimide GF 109203X is a potent and selective inhibitor of protein kinase C. J Biol Chem 1991;266:15771–81.

Ujiie H, Sasaoka T, Izumi K, Nishie W, Shinkuma S, Natsuga K, et al. Bullous pemphigoid autoantibodies directly induce blister formation without complement activation. J Immunol 2014;193:4415–28.

Watanabe M, Kosumi H, Osada SI, Takashima S, Wang Y, Nishie W, et al. Type XVII collagen interacts with the aPKC-PAR complex and maintains epidermal cell polarity. Exp Dermatol 2021;30:62−7.

Watanabe M, Natsuga K, Nishie W, Kobayashi Y, Donati G, Suzuki S, et al. Type XVII collagen coordinates proliferation in the interfollicular epidermis. Elife 2017;6:e26635.

Yin H, Han S, Cui C, Wang Y, Li D, Zhu Q. Plectin regulates Wnt signaling mediated-skeletal muscle development by interacting with Dishevelled-2 and antagonizing autophagy. Gene 2021;783:145562.

Zuidema A, Wang W, Sonnenberg A. Crosstalk between cell adhesion complexes in regulation of mechanotransduction. Bioessays 2020;42: e2000119.

SUPPLEMENTARY MATERIALS

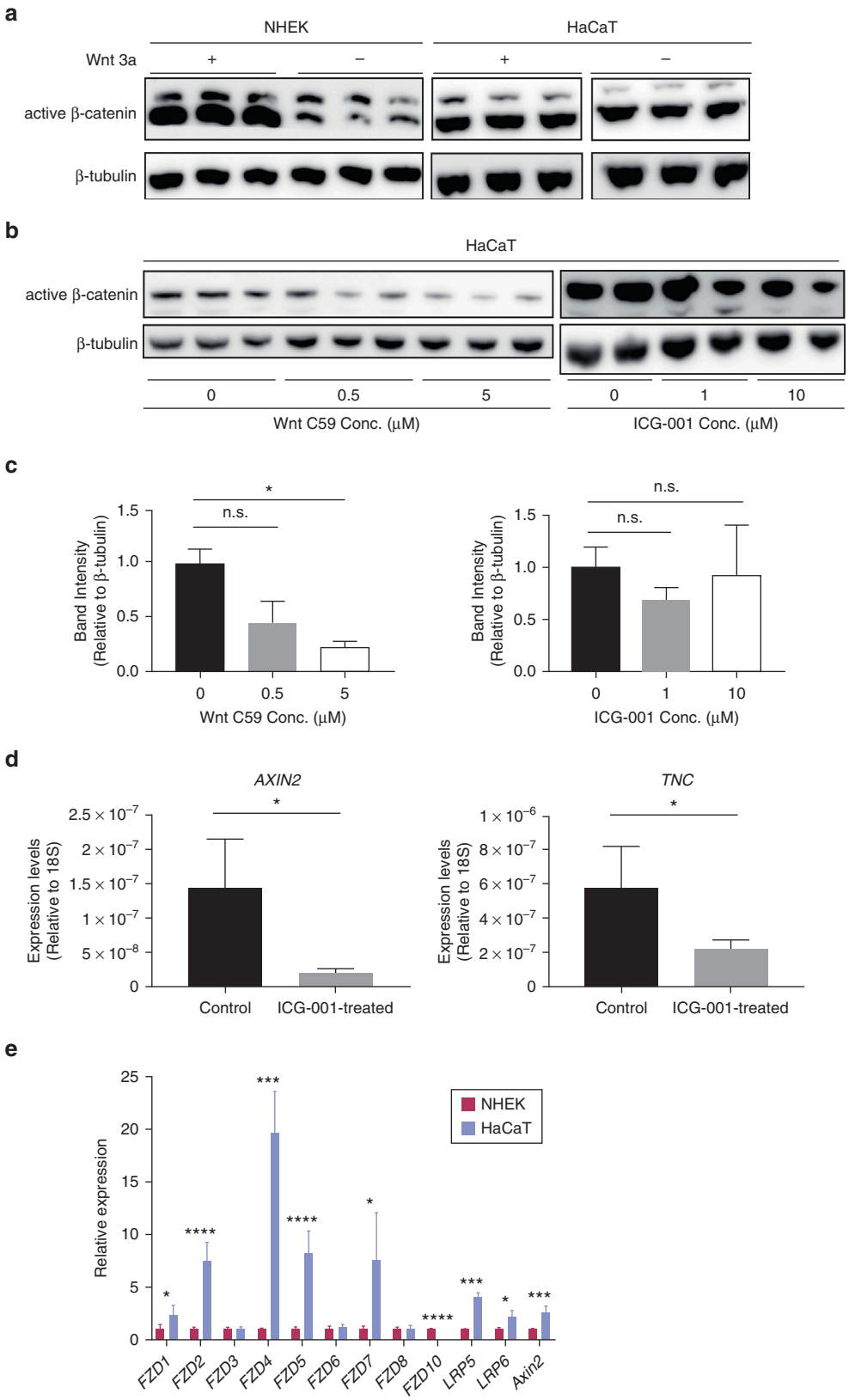

Supplementary Figure S1. Constitutive activation of canonical Wnt signaling in HaCaT cells. (**a**) Immunoblotting of nonphosphorylated β-catenin (Ser33/37/Thr41), the active form of β-catenin, in whole-cell lysates extracted from NHEKs and HaCaT cells. In HaCaT cells, β-catenin is constitutively activated without Wnt3a, showing the constitutive activation of canonical Wnt signaling. (**b**) Immunoblotting and (**c**) quantitative analysis of HaCaT cells treated with Wnt inhibitors (ICG-001 and Wnt C59). Active β-catenin is reduced with Wnt C59 in a dose-dependent manner, but the reduction is not evident with ICG-001. n = 5. Dunn's multiple comparison test. *0.01 < P < 0.05. (**d**) QRT-PCR of Wnt-target genes after Wnt inhibitor ICG-001 treatment in HaCaT cells. n = 3. Student's t-test. (**e**) QRT-PCR of Wnt-related molecules in HaCaT cells and NHEK. Gene expression of most Wnt receptors and AXIN2, a key regulator of canonical Wnt signaling, is upregulated in HaCaT cells. Representative images are shown from three or more replicates from each group. n = 3. The data are presented as means ± SE. Student's t-test. *0.01 < P < 0.05, ***0.0001 < P < 0.001, ****P < 0.0001. conc., concentration; NHEK, normal human epidermal keratinocyte; n.s., not significant; SE, standard error.

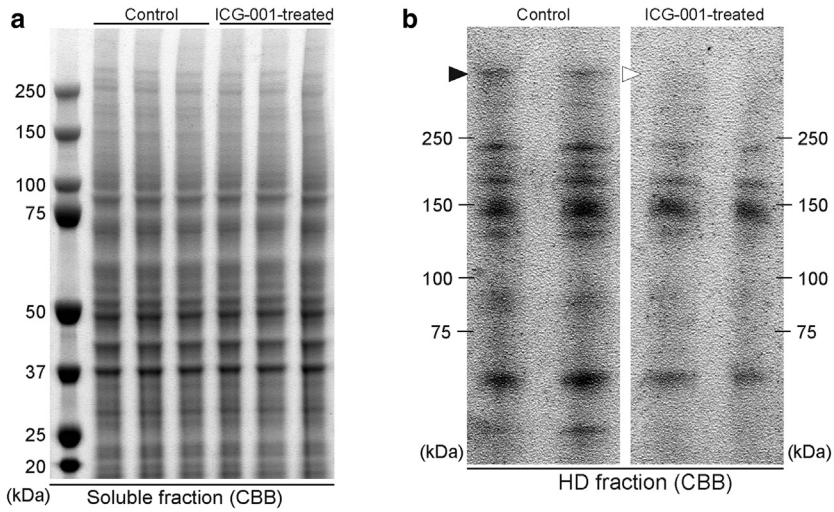

Supplementary Figure S2. Soluble and HD-rich fractions of Wnt-inhibited HaCaT cells using ICG-001. (**a**) CBB staining of ICG-001–treated HaCaT cell soluble fractions. (**b**) CBB staining of ICG-001–treated HaCaT cell HD-rich fractions. ICG-001 does not significantly alter soluble fraction proteins but reduces the intensity of the band above 250 kDa (arrowhead in **b**) in HD-rich fractions. Representative images are shown from three or more replicates from each group. CBB, coomassie brilliant blue; HD, hemidesmosome.

Supplementary Table S1. Primers Used in QRT-PCR

Gene Name	Forward (5′→3′)	Reverse (5′→3′)
FZD1	GAAAGTGCAGTGTTCCGCTG	CGAACTTGTTCATGAGCGCC
FZD2	CCGTGCCGCTCTATCTGTG	GTCCTCGGAGTGGTTCTGGC
FZD3	ACCTGACTTATGGAGCACTTGT	ACCACATTCCCAAACCACAG
FZD4	TTTCACACCGCTCATCCAGT	ATGGGCCAATGGGGATGTTG
FZD5	GGGATCCGTGGAGAGTCCTT	GGCAACCTGTTGGTTGCTTT
FZD6	TTTAGAGCCAGCGCCAAGAG	TCCTCAGAAGATCCCCATCCA
FZD7	TGAACAAGTTCGGCTTCCAGT	TAGGGCGCGGTAGGGTAG
FZD8	GGAGTGGGGTTACCTGTTGG	GTAGCCGATGCCCTTACACA
FZD10	GCTCAAGTGCTCCCCGATTA	GCCTCCATGCACAGGTAGTT
LRP5	ACCTGCTTGTCAGAGGCAC	TGAAGAAGCACAGGTGGCTG
LRP6	AACGCGAGAAGGGAAGATGG	ATCGCAAGTCCCGTCTGTTT
AXIN2	CCCCTCAGAGCGATGGATTT	AGTTGCTCACAGCCAAGACA
18S	GGCGCCCCCTCGATGCTCTTAG	GCTCGGGCCTGCTTTGAACACTCT
YWHAZ	ACTTTTGGTACATTGTGGCTTCAA	CCGCCAGGACAAACCAGTAT
DST	CGATATACTGCCCTGGTCACTC	GCCCCATGTTCAGAAGTCTC
PPL	GCCATTGCCAAGCACATGAA	TTGGTCACACGCTCCTTCAG
PLEC	CACTGGAGATCCAGCGACAG	CACCGTCTGCATCTCCTCAG
COL17A1	TCAACCAGAGGACGGAGTCA	TCGACTCCCCTTGAGCAAAC
ITGB4	GAGGGAGGAAGAGGATGGCA	TCTTCACTGGGGCCTTCTTG
TGM1	CTCGAAGGCTCTGGGTTACAG	GTGTCACTGTTTCATTGCCTCC
TNC	AGCATCCGGACCAAAACCAT	CCGATGCCATCCAGGAAACT